

Review

Kinetic and mechanistic studies of the reactions of transition
metal-activated oxygen with inorganic substrates

Andreja Bakac*

Ames Laboratory and Chemistry Department, Iowa State University, Ames, IA 50011, United States

Received 2 November 2005; accepted 3 February 2006

Available online 10 March 2006

Contents

1. Introduction	2047
2. Reactions with water and H ⁺	2047
2.1. Hydroperoxo and peroxo complexes	2048
2.2. Aquachromyl(IV) ion, Cr _{aq} O ²⁺	2050
3. Reactions with halide ions	2050
3.1. Hydroperoxo complexes	2050
3.1.1. Oxidation of I [−]	2050
3.1.2. Oxidation of Br [−] versus disproportionation of metal hydroperoxides	2051
3.1.3. Reaction of L(H ₂ O)RhOOH ²⁺ with HOBr	2052
3.1.4. Mechanistic possibilities	2053
3.2. Superoxo complexes	2053
3.3. Oxidation of bromide by Cr _{aq} O ²⁺	2054
4. Reactions with transition metal complexes	2055
5. Cross-reactions between metal-oxo, hydroperoxo, and superoxo complexes	2056
6. Acid catalysis in reductions of metal-activated oxygen	2056
7. Conclusions	2057
Acknowledgements	2057
References	2057

Abstract

The intermediates generated in the process of oxygen activation at metal centers participate in hydrogen and oxygen atom transfer, electron transfer, substitution, acid–base chemistry, and free radical chemistry. The reactivity and intrinsic lifetimes of such intermediates in aqueous solutions are a strong function of pH as the metal–oxygen interaction adds an extra dimension to the already complex pH dependence of O₂ reduction. Acid–base chemistry at “nonparticipating” ligands plays a major role in the kinetics and mechanisms, and can even determine the outcome of some reactions. Superoxometal complexes are subject to homolytic metal–oxygen bond cleavage in acidic solutions, but decompose by heterolysis at higher pH. Reactions of halides by hydroperoxo and peroxo complexes proceed through two major channels – oxidation of halide ions, and catalysis of H₂O₂ disproportionation – in close resemblance to enzymes haloperoxidases. The combination of the thermodynamics of electron transfer and protonation equilibria make transition metal hydroperoxo complexes both better oxidants and better reductants than the parent H₂O₂ in 2-electron reactions.

© 2006 Elsevier B.V. All rights reserved.

Keywords: Oxygen activation; Hydroperoxo; Oxygen transfer; Acid catalysis; Electron transfer; Halide

Abbreviations: ABTS^{2−}, 2,2′-azino-bis(3-ethylbenzothiazoline-6-sulfonic acid), diammonium salt; dppe, ethane-1,2-diylbis(diphenylphosphan); kie, kinetic isotope effect; L¹, 1,4,8,11-tetraazacyclotetradecane; L², *meso*-5,7,7,12,14,14-hexamethyl-1,4,8,11-tetraazacyclotetradecane; N4Py, *N*-[bis(2-pyridyl)methyl]-*N,N*-bis(2-pyridylmethyl)amine; phen, 1,10-phenanthroline; pz, pyrazine; Tp^{iPr}, hydrotris(3,5-di-2-propylpyrazolyl)borate

* Tel.: +1 515 294 3544; fax: +1 515 294 5233.

E-mail address: bakac@ameslab.gov.

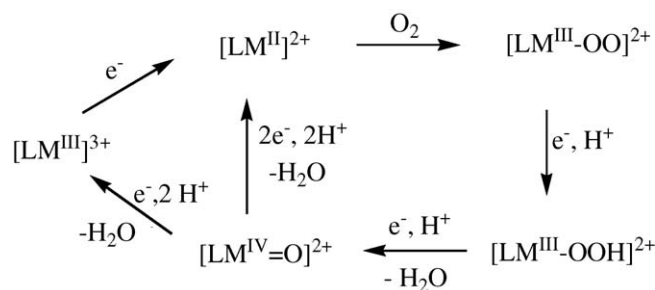
1. Introduction

Transition metal-catalyzed oxidation reactions with molecular oxygen and hydrogen peroxide in biological, industrial, and laboratory processes involve a plethora of intermediates of various lifetimes, reactivities, and roles. As a result, the chemistry of oxygen activation is a vibrant and extremely active field of investigation [1–11]. A different aspect of oxidation is found in processes that cause oxidative stress, aging and disease in plants and animals, deterioration of materials, and changes in the environment [12–16]. The discovery, identification, and synthesis of antioxidants, their structural determination, and analytical and mechanistic chemistry are thus also a focus of active research [17–22]. Still another area, generation of molecular oxygen in photosystem II, also fits the same general category in that transition metals, radicals, and various oxidation states of oxygen are involved [23–28].

These fields have, obviously, different goals. One seeks to improve oxidation processes, another to prevent them or to undo their outcome, and the third to generate molecular oxygen by oxidation of water. Perhaps it is not obvious that significant overlap should exist between these efforts, but the chemistry and intermediates involved are often remarkably similar. The intermediates – free radicals, and metals and oxygen in various oxidation states and degrees of association – participate in hydrogen and oxygen atom transfer, electron transfer, substitution and acid–base chemistry, formation of carbon and heteroatom radicals, and interaction of such radicals with each other and with various substrates. It would be all but impossible to provide even the most superficial survey of this enormous field and research effort in one place, but numerous books and review articles cover various areas and aspects of oxygen reactivity, as shown in the small selection of examples quoted above.

This review will focus on the kinetic and mechanistic aspects of the reactions of inorganic substrates with several forms of transition metal-activated oxygen. Special attention will be given to reactions with solvent and hydrogen ions, i.e. two reagents that often determine intrinsic lifetimes of superoxo, oxo, and hydroperoxo complexes as the simplest representatives and often well-defined forms of activated oxygen in model chemistry. Reactions with halides also will be presented in some detail, because these reactions have generated some extremely useful and revealing mechanistic information, and also because such chemistry may be directly relevant to biological systems. Hypohalites, halide ions, and various oxygen-derived intermediates occur and interact with each other and with their environment in natural systems, and also can be generated from therapeutic drugs. Fundamental understanding of such chemistry is thus necessary in order to develop means to predict, prevent, or emphasize its consequences, as appropriate, in various situations.

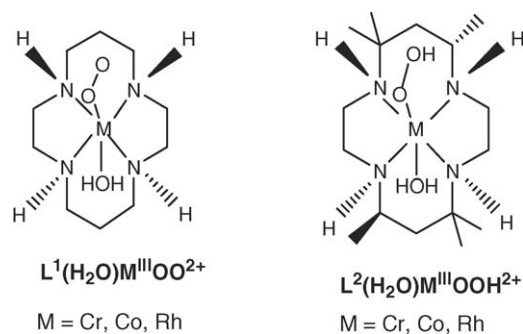
Reactions of activated oxygen with transition metal complexes will be given only a limited coverage because most of that chemistry has been reviewed previously [29]. Also, interactions of coordinated oxygen with nitrogen oxides, especially with NO, and the chemistry of the peroxynitrito and peroxyni-



Scheme 1.

trato complexes so formed [30–36] constitute a large and active area of research that has been continuously reviewed over the past decade [37–42] and will not be discussed here.

Structures of two of the most frequently mentioned types of macrocyclic complexes in this review are shown below.

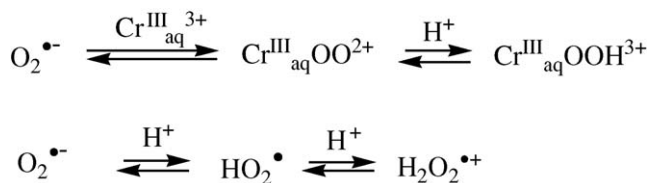


The sequence of events in Scheme 1 for (catalytic) activation of oxygen at a single metal center is a useful starting point, even though in a practical world the catalysis almost certainly could not be sustained; cross-reactions of various intermediates would quickly exhaust the system. Individual steps shown in Scheme 1 have, however, guided our thinking and helped develop strategies for the preparation of most of the metal-based intermediates whose chemistry is described below.

Unless stated otherwise, the rate constants are given at 25 °C.

2. Reactions with water and H⁺

The requirement for H⁺ in the stoichiometric and thermodynamic sense as oxygen is reduced to water creates also a kinetic role for H⁺ at various stages of this process. Coordination of oxygen to metal ions inevitably adds another dimension and more complexity to the pH-rate profiles, so that the lifetimes and redox reactivity of various intermediates depend greatly on the concentration of free H⁺ in solution. The combination of metal and oxygen, and of their acid–base chemistry, sometimes generates an exceptionally reactive oxidant. An example is provided by Cr_{aq}OOH³⁺, a protonated superoxochromium(III) ion, which is a much stronger oxidant than the predominant form, Cr_{aq}OO²⁺, see later. The non-metallic analog of Cr_{aq}OOH³⁺ is the doubly protonated superoxide, H₂O₂^{•+}, which should be a potent oxidant itself, but there is no evidence, spectral or kinetic, for such a species in solution under normal laboratory conditions. This example underlines one of the sometimes ignored roles of



Scheme 2.

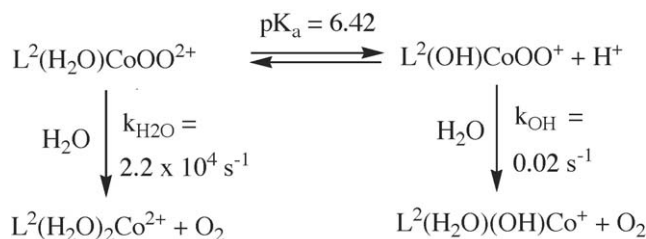
metal ions in oxygen activation, i.e. their effect on protonation equilibria at oxygen.

The acid–base equilibria of free and coordinated superoxide are shown in Scheme 2. Thermodynamically, $\text{Cr}_{\text{aq}}\text{OO}^{2+}$ is a weaker oxidant than HO_2^{\bullet} (although, in a practical sense, the much longer lifetime of $\text{Cr}_{\text{aq}}\text{OO}^{2+}$ makes it a competent oxidant). At the next protonation level, the thermodynamic advantage of the free species, $\text{H}_2\text{O}_2^{\bullet +}$, is rendered kinetically unimportant by its extreme acidity and, thus, low concentrations. The metallic analog, $\text{Cr}_{\text{aq}}\text{OOH}^{3+}$, is also a minor, spectroscopically unobserved species, but kinetically relevant concentrations must be present at $\text{pH} \leq 1$ if this species is indeed responsible for the H^+ -catalyzed oxidation by $\text{Cr}_{\text{aq}}\text{OO}^{2+}$, see later.

In some other cases, protonation of coordinated oxygen increases the redox reactivity, but simultaneously decreases intrinsic lifetimes of such species. Such behavior is often observed with the hydroperoxo complexes, such as $\text{Cr}_{\text{aq}}\text{OOH}^{2+}$, $\text{L}(\text{H}_2\text{O})\text{RhOOH}^{2+}$ ($\text{L} = \text{L}^1, \text{L}^2, (\text{NH}_3)_4$), or $\text{Co}(\text{CN})_5\text{OOH}^{3-}$, as discussed in detail below.

Acid–base chemistry at nonparticipating ligands also has a major influence on the lifetimes of various intermediates, and on the oxidation state of oxygen released in the decomposition process. Most notably for superoxo complexes, the chemistry in acidic solutions is often dominated by the homolysis of the metal–oxygen bond. This path is much less important at higher pH owing to the stabilization of the higher oxidation state by coordinated hydroxyl groups. As an illustration, the complex $\text{L}^2(\text{H}_2\text{O})\text{CoOO}^{2+}$ has $k_{\text{H}_2\text{O}} = 2.2 \times 10^4 \text{ s}^{-1}$ in acidic solutions ($\text{pH} < 5$), but the singly deprotonated form, $\text{L}^2(\text{OH})\text{CoOO}^+$, homolyzes more slowly by a factor of 10^6 , $k_{\text{OH}} = 0.02 \text{ s}^{-1}$ [43], Scheme 3.

Qualitatively similar observations were made with $\text{L}^2(\text{H}_2\text{O})\text{RhOO}^{2+}$, which decomposes readily in the absence of O_2 in acidic solutions, but can be deaerated safely at pH 11 [34,35]. Anions, such as chloride or thiocyanate also diminish homolysis rates of superoxo complexes, but the effect is not as dramatic as it is for the hydroxide, as shown in Table 1 [43,44].



Scheme 3.

Table 1
Effect of pH and anions on homolytic cleavage of $\text{Co}-\text{O}_2$ bond^a

Complex	$k_{\text{hom}} (\text{s}^{-1})$
$\text{L}^2(\text{H}_2\text{O})\text{CoOO}^{2+}$	2.2×10^4
$\text{L}^2(\text{Cl})\text{CoOO}^+$	3.3×10^3
$\text{L}^2(\text{SCN})\text{CoOO}^+$	17.7
$\text{L}^2(\text{OH})\text{CoOO}^+$	0.021

Data from Ref. [43,44].

^a In aqueous solutions at 25 °C.

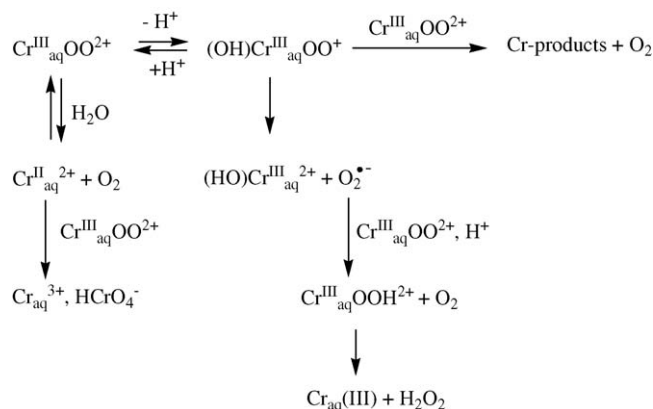
Metal– O_2 bond homolysis is a major step in the decomposition of $\text{Cr}_{\text{aq}}\text{OO}^{2+}$ in acidic solutions. This is followed by a complex, multistep reaction between $\text{Cr}_{\text{aq}}^{2+}$ and $\text{Cr}_{\text{aq}}\text{OO}^{2+}$ that eventually produces $\text{Cr}_{\text{aq}}^{3+}$ and HCrO_4^- . At higher pH, the decay rate increases. Based on the data and arguments presented above, and the lack of kinetic dependence on $[\text{O}_2]$ at $\text{pH} > 4$ [45], homolysis can be ruled out; another path must be gaining importance under those conditions.

As shown in Scheme 4, this is a case of pH-induced mechanistic changeover from homolytic to heterolytic $\text{Cr}-\text{O}_2$ bond cleavage. The conjugate base, $(\text{OH})\text{Cr}_{\text{aq}}\text{OO}^+$, reacts mainly by dissociation to $\text{Cr}_{\text{aq}}(\text{III})$ and free superoxide. Interestingly, this unimolecular process leads to disproportionation of coordinated superoxide to free O_2 and H_2O_2 . A parallel, bimolecular reaction between $\text{Cr}_{\text{aq}}\text{OO}^{2+}$ and $(\text{OH})\text{Cr}_{\text{aq}}\text{OO}^+$ generates O_2 , $\text{Cr}_{\text{aq}}(\text{III})$ and chromate.

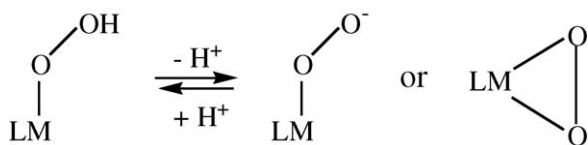
2.1. Hydroperoxo and peroxo complexes

Coordination of H_2O_2 to high-valent metal centers generates metal peroxo complexes that have the peroxo unit bound in a side-on fashion. In these molecules, peroxide is electrophilically activated and thus capable of oxidation of various substrates in both biological and industrial milieu [46–50].

Interaction of molecular oxygen with low valent transition metals usually generates reactive hydroperoxo species with the HOO -group bound end-on to an intermediate oxidation state of the metal, i.e. $\text{Co}(\text{III})$, $\text{Cr}(\text{III})$, $\text{Rh}(\text{III})$, etc. The best known functioning example is the active form of the antitumor agent bleomycin which has an $\text{Fe}^{\text{III}}-\text{OOH}^+$ unit at the active site [51,52].



Scheme 4.



Scheme 5.

The third class of peroxo compounds falls between the two extremes, and has a peroxo unit coordinated to metals in intermediate oxidation states, i.e. Fe(III) or Rh(III). Such complexes are generated by reversible deprotonation of the hydroperoxo unit, as shown in Scheme 5. Although the distinction between side-on versus end-on coordination of the peroxo unit is not always straightforward or easily made [53,54], experimental evidence often favors side-on binding [55,56]. The first example of side-ways bonding in a peroxo complex of a tetraaminecobalt(III) complex was reported recently [57].

An interesting situation was observed in the reaction of O₂ with a rhodium(I) complex, (Tp^{iPr})Rh(dppe) [55]. In the presence of pz^{iPr}H, the reaction yielded a side-on peroxo complex (Tp^{iPr})Rh(pz^{iPr}H)(O₂). Replacing pz^{iPr}H by the smaller, unsubstituted pyrazine generated an end-on hydroperoxo complex, (Tp^{iPr})Rh(pzH)(pz)(O₂H), derived from an initially formed peroxo complex, Scheme 6. The same sequence of events is believed to occur in the process of oxygen-activation by cytochrome P450 enzymes to generate the hydroperoxo form, which directly precedes the active oxidant, a porphyrin radical cation of Fe(IV) [1]. Experimental demonstration for this ordering of events was also provided for oxygenated myoglobin [58]. The initial formation of the peroxo-bound myoglobin at 77 K, and its conversion to the hydroperoxo derivative by proton transfer upon annealing to 185 K, were directly observed. Similarly, cryoradiolysis of the oxy-ferrous horseradish peroxidase at 77 K generates the peroxo ferric complex, which is again protonated at higher temperatures to give the hydroperoxo ferric species [59].

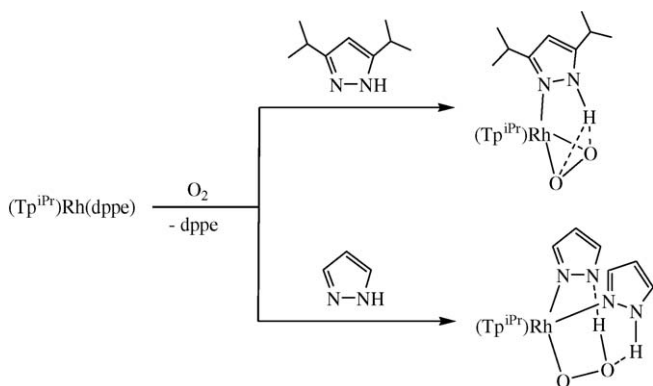
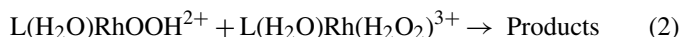
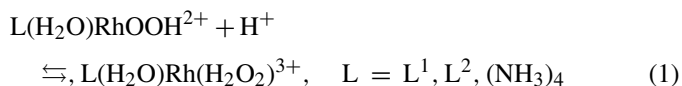
All the reported examples of the hydroperoxo/peroxo transformations have been observed in non-aqueous solutions [53–56,60,61]. For iron complexes, a dramatic color change is usually observed as the high spin peroxo species turns into the low-spin hydroperoxo form [62–65]. This chemistry is not limited to complexes of rhodium and iron, but has also been observed for other metals, such as copper [66,67] and palla-

dium [68]. In terms of reactivity, an interesting observation was reported for the Fe^{III}(N4Py) complexes; of the two forms, only the more electrophilic hydroperoxo species was capable of alkane hydroxylations [56].

The stability of the hydroperoxo complexes in aqueous solutions varies greatly with the metal and ligands. Solutions of L(H₂O)CoOOH²⁺ (L = L¹, L²) are quite persistent under acidic conditions [69,70], as one would expect for complexes of a substitutionally inert metal ion in a stable oxidation state. In the case of the L² complex, the lifetime was sufficiently long to obtain crystals for X-ray structure determination [70]. With an increase in the pH, however, these complexes decay more readily. At pH > 5, L²(H₂O)CoOOH²⁺ decomposes instantaneously [70], but the detailed kinetics or products of this reaction have not been determined.

The behavior exhibited by the rhodium analogues is different in that their stability is the greatest at high pH. In acidic solutions, these complexes decay by a mechanism that appears to involve disproportionation of the coordinated peroxide entity, although precise kinetics and product data are not available [71]. This pH profile is very different from that exhibited by free H₂O₂ which is quite stable in acid but disproportionates readily at higher pH. In general, disproportionation is one of the more common pathways for the decomposition of hydroperoxo complexes [72–75].

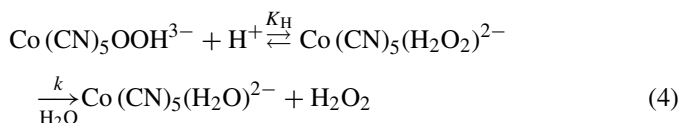
The much faster base hydrolysis of L(H₂O)CoOOH²⁺ than of L(H₂O)RhOOH²⁺ is precisely as expected on the basis of the known, well established pattern in which cobalt always reacts faster of the two. The rate constants for base hydrolysis of (NH₃)₅CoX²⁺ complexes, for example, are several orders of magnitude greater than those reported for the corresponding rhodium series [76,77]. It is surprising, however, that the disproportionation of L(H₂O)RhOOH²⁺ at pH ≤ 2 is so fast (minutes to hours) [71]. From the acid dependence, one infers that L(H₂O)RhOOH²⁺ and its protonated form are the reactive species, Eqs. (1) and (2). The data are insufficient to explain whether it is the lower abundance or lower reactivity of the protonated species that makes the cobalt complexes less reactive by this pathway.



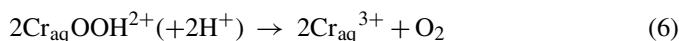
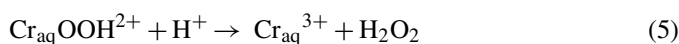
Scheme 6.

In contrast to the cationic cobalt complexes, the anionic Co(CN)₅OOH³⁻ decomposes by acid hydrolysis according to the rate law of Eq. (3), and the mechanism in Eq. (4), over the entire pH range studied, 3 < pH < 9 [78]. The data yielded the protonation equilibrium constant K_H = 1.5 × 10⁵ M⁻¹ (independent of temperature at 20–40 °C), and the rate constant for the aquation of the hydrogen peroxide complex, k = 1.89 × 10⁻² s⁻¹ at 20 °C, and 0.135 s⁻¹ at 40 °C. A conservative estimate places the upper limit for the aquation rate constant for the hydroperoxo species, Co(CN)₅OOH³⁻, at < 5 × 10⁻⁶ s⁻¹ [78].

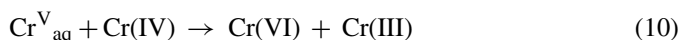
$$\frac{-d[\text{Co(CN)}_5\text{OOH}^{3-}]}{dt} = \frac{kK_H[\text{Co(CN)}_5\text{OOH}^{3-}][\text{H}^+]}{1 + K_H[\text{H}^+]} \quad (3)$$



Both the kinetics and products of the decay of $\text{Cr}_{\text{aq}}\text{OOH}^{2+}$ are affected by the concentrations of H^+ and of the hydroperoxo complex [74]. Kinetic traces are approximately first-order at low concentrations of $\text{Cr}_{\text{aq}}\text{OOH}^{2+}$, but additional terms become important, and the lifetime of $\text{Cr}_{\text{aq}}\text{OOH}^{2+}$ decreases, at higher initial concentrations. The reaction generates mixtures of H_2O_2 , O_2 , $\text{Cr}_{\text{aq}}^{3+}$ and HCrO_4^- . These results were interpreted [74] by invoking three simultaneous pathways, Eqs. (5)–(7), whose relative contributions change with reaction conditions. The yields of H_2O_2 increase with $[\text{H}^+]$, which suggests acidolysis as a major H_2O_2 -generating pathway, Eq. (5). Disproportionation of the hydroperoxo moiety is the proposed source of O_2 , and disproportionation involving the metal and hydroperoxide is the source of chromate.



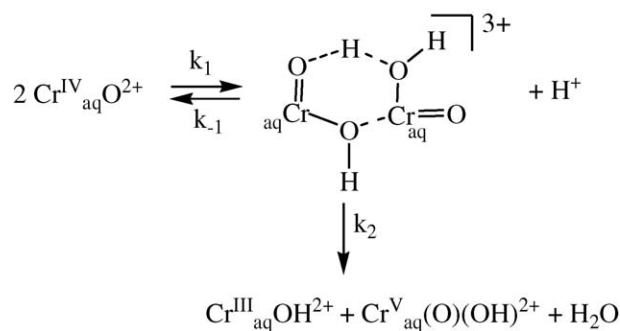
One can draw a reasonably straightforward mechanistic picture for reactions (5) and (6), but reaction (7) is accompanied by major changes in the degree of hydrolysis, coordination number, and geometry around the metal. Almost certainly, this is a multistep process featuring Cr(V) and/or Cr(IV) as intermediates. The lack of detailed kinetic information makes it difficult to propose a mechanism, but several possibilities present themselves, including an initial intramolecular electron transfer from metal to the hydroperoxo group to yield Cr(V), followed by disproportionation to the observed products, Cr(III) and Cr(VI), Eqs. (8)–(10). The hydrolytic state or coordination number for Cr(V) is not known, although the species produced by one-electron reduction of chromate in acidic solutions was proposed to exist as a mixture of H_3CrO_4 ($\text{p}K_a = 2.7$), H_2CrO_4^- ($\text{p}K_a = 3.8$) and HCrO_4^{2-} [79].



The chemistry analogous to that in Eq. (8) has been observed with $\text{L}(\text{H}_2\text{O})\text{CrOOH}^{2+}$ ($\text{L} = \text{L}^1, \text{L}^2$) [80–83] in which case the reaction is facilitated by electron donation from the N_4 macrocyclic ligands. It will be certainly more difficult to generate Cr(V) in the absence of stabilizing ligands, but this is true regardless of whether the reaction employs the mechanism of Eq. (8) or a different one. Detailed kinetic studies will be critical in addressing the mechanism of reaction (7).

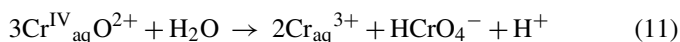
2.2. Aquachromyl(IV) ion, $\text{Cr}_{\text{aq}}\text{O}^{2+}$

The most outstanding feature of the disproportionation, Eq. (11), is a large solvent kinetic isotope effect, $k_H/k_D = 6.9$, sug-



Scheme 7.

gesting the cleavage of an O–H bond in the rate determining step [84]. This mechanism bears close resemblance to the proposed hydrogen atom abstraction by tyrosine radicals [85–87] from manganese-coordinated O–H in Photosystem II.



The reaction is second-order in $[\text{Cr}_{\text{aq}}\text{O}^{2+}]$ and inversely first-order in $[\text{H}^+]$, Eq. (12).

$$\frac{-d[\text{Cr}_{\text{aq}}\text{O}^{2+}]}{dt} = 38.8 [\text{Cr}_{\text{aq}}\text{O}^{2+}]^2 [\text{H}^+]^{-1} \quad (12)$$

All the experimental observations are consistent with a bridged transition state/intermediate of the kind shown in Scheme 7 followed by disproportionation of Cr(V) or by the Cr(V)/ $\text{Cr}_{\text{aq}}\text{O}^{2+}$ reaction, as shown in Eqs. (9) and (10). Interestingly, the formation of HCrO_4^- was somewhat slower than the disappearance of $\text{Cr}_{\text{aq}}\text{O}^{2+}$, suggesting the involvement of persistent intermediate(s).

3. Reactions with halide ions

In the mechanistic sense, oxidation of halides turned out to be especially revealing because several forms of metal-activated oxygen (superoxo, hydroperoxo, and oxo) reacted with either iodide or bromide, or both, which made it possible to map out and gauge the reactivity of various forms relative to each other, as well as to examine the effect of the metal and non-participating ligands on reactivity.

3.1. Hydroperoxo complexes

3.1.1. Oxidation of I^-

In terms of kinetics and stoichiometry, the behavior of the hydroperoxides is the most straightforward. Oxidation of I^- by the rhodium complexes, $\text{L}(\text{H}_2\text{O})\text{RhOOH}^{2+}$ ($\text{L} = \text{L}^1, \text{L}^2, (\text{NH}_3)_4$) takes place according to the stoichiometry of Eqs. (13) and (14) and follows the third-order rate law of Eq. (15) [88].

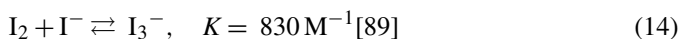
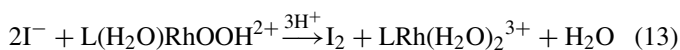


Table 2

Kinetic data for the reactions of metal hydroperoxides with halide ions and with HOBr^a

LMOOH ²⁺	k_I^b	k_{Br}^b	k_{HOBr}^c	Reference
(H ₂ O) ₅ CrOOH ²⁺	988 (16) ^d	0.54 ^e	9.5×10^{6f}	[88,90]
L ¹ (H ₂ O)CoOOH ²⁺	100 (2) ^d			[90]
L ² (H ₂ O)CoOOH ²⁺	72.3 (21) ^d			[90]
(NH ₃) ₄ (H ₂ O)RhOOH ²⁺	8800 (60) ^g	2.35 (5) ^g	3×10^{8h}	[88]
		1.8 ^h		[88]
L ¹ (H ₂ O)RhOOH ²⁺	536 (7) ^g	0.200 (1) ^h		[88]
L ² (H ₂ O)RhOOH ²⁺	530 (11) ^g	0.55 (2) ⁱ		[88]
H ₂ O ₂	0.173 ^j	0.00023 ^k	$(1.5-5.8) \times 10^4$	[91–93]

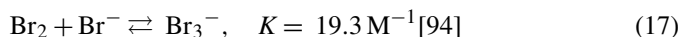
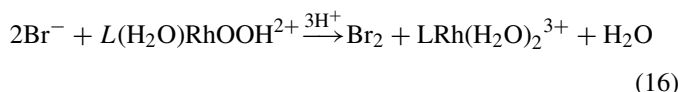
^a Aqueous solutions, 25 °C. Numbers in parentheses represent one standard deviation of the last significant figure.^b k in M⁻² s⁻¹.^c k in M⁻¹ s⁻¹.^d Ionic strength (μ) 0.075 M.^e μ = 2.0 M.^f μ = 0.50 M.^g μ = 0.10 M.^h μ = 1.0 M.ⁱ μ = 0.20 M.^j [H⁺]-independent term has $k_0 = 0.0115$ M⁻¹ s⁻¹.^k [H⁺]-independent term has $k_0 = 3.8 \times 10^{-7}$ M⁻¹ s⁻¹. Reproduced with permission from *Inorg. Chem.* 2004, 43, 4505–4510. © 2004 Am. Chem. Soc.

$$\frac{-d[L(H_2O)RhOOH^{2+}]}{dt} = k_I[L(H_2O)RhOOH^{2+}][H^+][I^-] \quad (15)$$

Kinetic data are summarized in Table 2. Unlike the reactions of halides with H₂O₂, the oxidation with metal hydroperoxides examined here exhibit no acid independent terms. The most reasonable mechanism involves oxygen atom transfer from the protonated hydroperoxide to iodide, followed by the known, rapid comproportionation reaction between HOI and I⁻ to generate the observed product, I₂/I₃⁻.

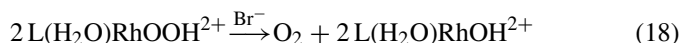
3.1.2. Oxidation of Br⁻ versus disproportionation of metal hydroperoxides

At reasonably high acid (>0.1 M) and bromide (>0.01 M) concentrations, the L(H₂O)RhOOH²⁺/Br⁻ reaction is acid-catalyzed and produces bromine, similar to the iodide case described above, Eqs. (16) and (17).



The yields of bromine are, however, quantitative only at the highest [H⁺] (ca 1 M) and [Br⁻] (0.1 M) used. With decreasing concentrations of both of these reagents, the diminishing yields of bromine are accompanied by increasing production of molecular oxygen, which becomes the sole product at <0.1 M H⁺ and <0.01 M Br⁻. The role of Br⁻ has changed from that of a reductant at high acid and bromide concentrations to that of a catalyst for the disproportionation of coordinated hydroperoxide at low [H⁺] and [Br⁻], Eq. (18). The change in the chemistry is accompanied by dramatic changes in the appearance of kinetic traces. The absorbance in the UV increases in the high H⁺, Br⁻ regime, as the strongly absorbing Br₃⁻ is generated. At the other extreme, i.e. at low concentrations of H⁺ and Br⁻, the

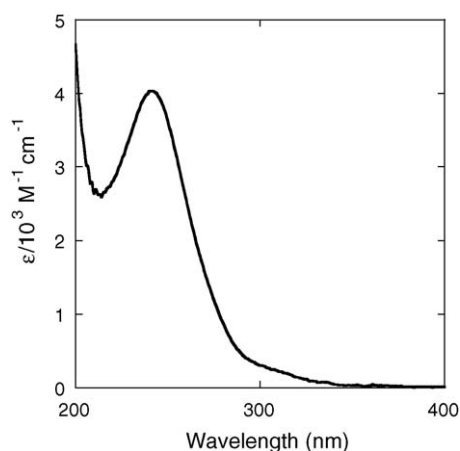
absorbance in the UV decreases because the disappearance of L(H₂O)RhOOH²⁺ (spectrum shown in Fig. 1) leads to the formation of less-absorbing products. This behavior is illustrated in Fig. 2.



Under all the conditions used, the data obeyed the third-order rate law of Eq. (19). The kinetic order with respect to every reactant remained unchanged throughout, but the numerical value of the rate constant changed by a factor of about two between the two extremes, $1 < n < 2$ [88] as shown in Fig. 3.

$$\frac{-d[L(H_2O)RhOOH^{2+}]}{dt} = n k_{Br}[L(H_2O)RhOOH^{2+}][H^+][Br^-] \quad (19)$$

The data were rationalized by the mechanism in Scheme 8, according to which the hydrolysis of bromine, followed by rapid

Fig. 1. UV spectrum of (NH₃)₄(H₂O)RhOOH²⁺ in 0.10 M HClO₄.

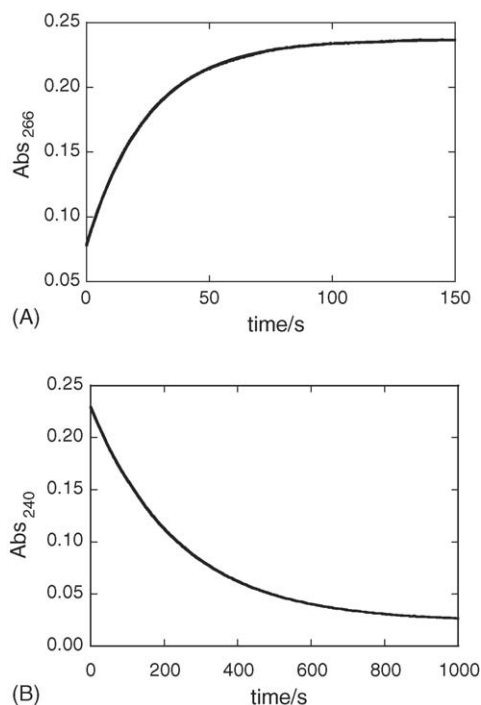


Fig. 2. Kinetic traces for the reaction of $(\text{NH}_3)_4(\text{H}_2\text{O})\text{RhOOH}^{2+}$ with Br^- under two sets of conditions. Panel A: 0.98 M H^+ , 0.020 M Br^- , $0.025 \text{ mM } (\text{NH}_3)_4(\text{H}_2\text{O})\text{RhOOH}^{2+}$; absorbance increases at the 266 nm maximum of $\text{Br}_2/\text{Br}_3^-$. Panel B: 0.09 M H^+ , 0.010 M Br^- , $0.06 \text{ mM } (\text{NH}_3)_4(\text{H}_2\text{O})\text{RhOOH}^{2+}$; absorbance decreases at the 240 nm maximum of the rhodium complex.

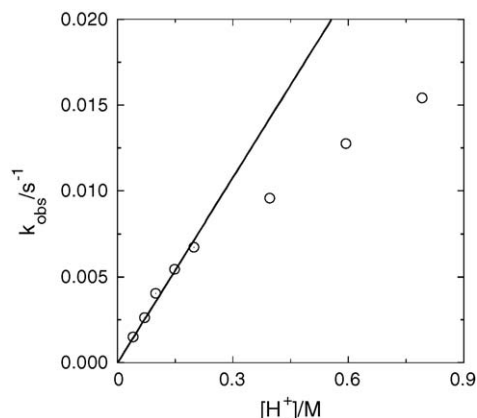
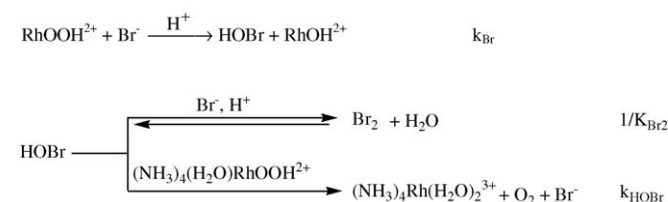
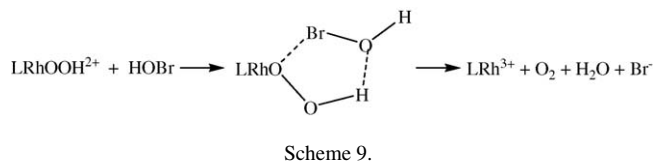


Fig. 3. Plot of k_{obs} vs. $[\text{H}^+]$ for the oxidation of Br^- (10 mM) with $(\text{NH}_3)_4(\text{H}_2\text{O})\text{RhOOH}^{2+}$ ($5 \times 10^{-5} \text{ M}$) at 25°C and 1.0 M ionic strength. The slope at the highest concentration of H^+ is twice as large as the slope at low $[\text{H}^+]$. Reproduced with permission from *Inorg. Chem.* 2004, 43,4505–4510. © 2004 Am. Chem. Soc.



Scheme 8.



oxidation of $\text{L}(\text{H}_2\text{O})\text{RhOOH}^{2+}$, is responsible for the observed behavior.

Subsequently, the $\text{HOBr}/\text{L}(\text{H}_2\text{O})\text{RhOOH}^{2+}$ reaction was examined directly for $\text{L} = (\text{NH}_3)_4$, as follows.

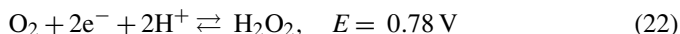
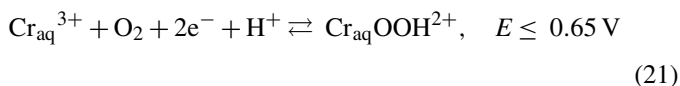
3.1.3. Reaction of $\text{L}(\text{H}_2\text{O})\text{RhOOH}^{2+}$ with HOBr

The rate law of Eq. (20) was established, where k represents the product of the equilibrium constant for hydrolysis of Br_2 ($K_{\text{Br}_2} = 6.1 \times 10^{-9} \text{ M}^{-2}$) and the rate constant for the oxidation of $(\text{NH}_3)_4(\text{H}_2\text{O})\text{RhOOH}^{2+}$ by HOBr , k_{HOBr} . The data yielded $k_{\text{HOBr}} = 2.9 \times 10^8 \text{ M}^{-1} \text{ s}^{-1}$.

$$\begin{aligned}
 & -\frac{d[(\text{NH}_3)_4(\text{H}_2\text{O})\text{RhOOH}^{2+}]}{dt} \\
 &= \frac{k[(\text{NH}_3)_4(\text{H}_2\text{O})\text{RhOOH}^{2+}][\text{Br}_2]}{[\text{H}^+][\text{Br}^-]} \quad (20)
 \end{aligned}$$

Analogous chemistry also plays a role in the $\text{Cr}_{\text{aq}}\text{OOH}^{2+}/\text{Br}^-$ reaction, where $k_{\text{HOBr}} = 9.5 \times 10^6 \text{ M}^{-1} \text{ s}^{-1}$. Although smaller than in the case of the rhodium complex, this rate constant is still much greater than that for free H_2O_2 , for which the reported values lie in the range $(1.5\text{--}5.8) \times 10^4 \text{ M}^{-1} \text{ s}^{-1}$ [91–93].

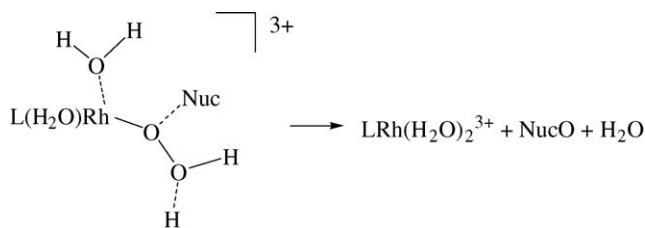
On the basis of the limited potential data for $\text{Cr}_{\text{aq}}\text{OOH}^{2+}$, the difference in rate constants appears to be thermodynamic in origin, Eqs. (21) and (22). The estimated 0.13 V difference in 2-e potentials is equivalent to a ΔG^0 that is by 25 kJ/mol more favorable for the chromium reaction, and that might reasonably result in several hundred-fold greater rate constant k_{HOBr} for $\text{Cr}_{\text{aq}}\text{OOH}^{2+}$:



In the absence of potential data, similar analysis cannot be carried out for $\text{L}(\text{H}_2\text{O})\text{RhOOH}^{2+}$. If, however, the 30-fold greater value of k_{HOBr} for $(\text{NH}_3)_4(\text{H}_2\text{O})\text{RhOOH}^{2+}$ is the result of changed thermodynamics, then the data can be used to estimate the potential for the rhodium couple in the equivalent of reaction (21) as $\sim 0.1 \text{ V}$ lower than that for the chromium, i.e. $E_{\text{Rh}} \leq 0.55 \text{ V}$.

The proposed mechanism for the oxidation of metal hydroperoxides by HOBr is analogous to that suggested earlier [95] for the reaction of free H_2O_2 , i.e. nucleophilic attack by hydroperoxide at the bromine site in HOBr , as shown in Scheme 9.

In a broader context, the oxidation of halide ions with metal hydroperoxo and peroxo complexes is closely related to that exhibited by haloperoxidases, enzymes that catalyze the



Scheme 10.

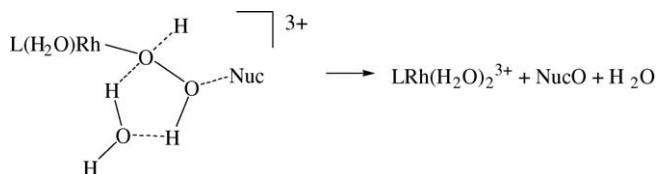
oxidation of organic substrates with halides, and disproportionation of H_2O_2 to oxygen and H_2O [96]. Bromide oxidation is accelerated by H^+ both in the enzymatic systems [96] and in some functional models, such as oxoperoxovanadium(V) complexes [97]. Acid catalysis does not, however, appear to be a standard feature in oxidation reactions by peroxo complexes [92], although the number of studies focusing on pH dependence may be too small to offer a definitive picture at the present time [96].

3.1.4. Mechanistic possibilities

Probably the most intriguing mechanistic issue concerning the oxidation of halides by hydroperoxo complexes is the site of initial nucleophilic attack [98]. The protonation at the adjacent oxygen, i.e. that bound directly to the metal, is believed to lead to the dissociation of peroxide from the metal. This site of attack therefore would not be expected to play a role in oxygen atom transfer. Protonation at the remote oxygen, on the other hand, would both create H_2O , an excellent leaving group, and enable transfer of adjacent oxygen to the nucleophile, as shown in Scheme 10.

An alternative mechanism, attack at the remote oxygen in Scheme 11, cannot be totally dismissed, however, especially for the cationic hydroperoxo complexes of rhodium, which are not subject to acidolysis under normal conditions [98]. The failure of H_2O_2 to dissociate from the rhodium may mean that protonation at the adjacent oxygen does not take place, or that the coordinated hydrogen peroxide does not dissociate as readily from $\text{L}(\text{H}_2\text{O})\text{Rh}(\text{H}_2\text{O}_2)^{3+}$ and from other substitutionally inert complexes as it does from more labile metal ions. In support of this idea, note that the dissociation of H_2O_2 from $\text{Co}(\text{CN})_5(\text{H}_2\text{O}_2)^{2+}$ is not instantaneous, $k = 1.89 \times 10^{-2} \text{ s}^{-1}$ at 20°C [78].

In Scheme 11, the protonation is pictured as taking place at the more electron-rich adjacent oxygen, while the nucleophile attacks at the more accessible remote site. In concert with O-transfer to nucleophile, the proton shifts between the two oxygen atoms in a process that is assisted by a molecule of hydrogen-bonded water. This mechanism, or a variant, seems attractive for the reactions of sterically encumbered nucleophiles, such as triphenylphosphine [98].



Scheme 11.

Table 3

Summary of kinetic data for acid-catalyzed oxidation reactions of I^- by $\text{L}(\text{H}_2\text{O})\text{MOO}^{2+}$ ^a

Complex	$k_t (\text{M}^{-2} \text{s}^{-1})$
$\text{Cr}_{\text{aq}}\text{OO}^{2+}$	93.7
$\text{Cr}_{\text{aq}}\text{OO}^{2+}$	185 ^b
$\text{L}^1(\text{H}_2\text{O})\text{CrOO}^{2+c}$	402
$(\text{NH}_3)_4(\text{H}_2\text{O})\text{RhOO}^{2+}$	888

^a Acidic aqueous solutions, 25°C .

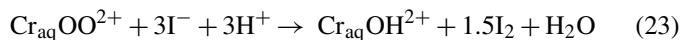
^b In D_2O , calculated from data at 0.10 M DClO_4 .

^c $\text{L}^1 = [14]\text{aneN}_4$.

The data in Table 2 underscore an important effect of coordination on peroxide reactivity, i.e. the metal-complexed hydroperoxide is more reactive than H_2O_2 as both an oxidant and a reductant. As discussed in the reactions with HOBr , the better reducing properties are clearly a thermodynamic effect. On the other hand, the faster oxidation reactions seem to run contrary to the driving force. These data can be rationalized by noting that the reactions in Table 2 were run in acidic solutions, and that the difference in equilibrium concentrations of the protonated forms, $\text{LM}(\text{H}_2\text{O}_2)^{3+}$ and H_3O_2^+ , may be responsible for the observed pattern. The aqueous pK_a for the “exceptionally powerful oxidant,” H_3O_2^+ , has been estimated to lie below -7.7 [99]. No credible data are available for $\text{LM}(\text{H}_2\text{O}_2)^{3+}$ complexes, although a K_a of 0.06 M has been calculated for $\text{Fe}(\text{H}_2\text{O})_5\text{H}_2\text{O}_2^{3+}$ from the kinetic data for the decomposition of H_2O_2 at exceptionally high concentrations [100].

3.2. Superoxo complexes

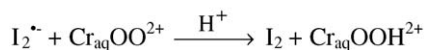
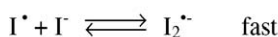
Oxidation of iodide by $\text{L}(\text{H}_2\text{O})\text{MOO}^{2+}$ ($\text{L} = (\text{H}_2\text{O})_5$, L^1 ; $\text{M} = \text{Cr}, \text{Rh}$) exhibited a 3:1 $[\text{I}^-]/[\text{L}(\text{H}_2\text{O})\text{MOO}^{2+}]$ stoichiometry and utilized only an acid-catalyzed path in the redox step of Eqs. (23) and (24) [101], which was followed by the I_2/I_3^- equilibration.



$$\frac{-d[\text{Cr}_{\text{aq}}\text{OO}^{2+}]}{dt} = \frac{2}{3} \frac{d[\text{I}_2]}{dt} = k_{\text{Cr}}[\text{Cr}_{\text{aq}}\text{OO}^{2+}][\text{I}^-][\text{H}^+] \quad (24)$$

Kinetic data are summarized in Table 3. An inverse solvent kinetic isotope effect, believed to be a feature of all the reactions in Table 3, was demonstrated in the $\text{Cr}_{\text{aq}}\text{OO}^{2+}/\text{I}^-$ reaction, $k_{\text{H}}/k_{\text{D}} = 0.5$. A comparable value was obtained in the corresponding reaction of the hydroperoxo complex, $k_{\text{H}}/k_{\text{D}} = 0.6$ [101]. All the data, including the inverse kie, implicate a protonated superoxo complex as the reactive form. The greater acidity of $\text{Cr}_{\text{aq}}\text{OOH}^{3+}$ than of $\text{Cr}_{\text{aq}}\text{OOD}^{3+}$, i.e. the smaller proportion of the protonated form in equilibrium with the unprotonated dication, results in the lower overall reaction rate in H_2O .

The two major mechanistic possibilities for the $\text{L}(\text{H}_2\text{O})\text{MOO}^{2+}/\text{I}^-$ reactions are shown for the $\text{Cr}_{\text{aq}}\text{OO}^{2+}$ case in Schemes 12 and 13. In both cases, the rate-determining step is followed by thermodynamically favorable, rapid steps leading to the final products.



Scheme 12.

The one-electron path generates the metal hydroperoxide and iodine atom, followed by the $\text{Cr}_{\text{aq}}\text{OOH}^{2+}/\text{I}^-$ reaction described in the previous section, and the independently confirmed reduction of an additional equivalent of $\text{Cr}_{\text{aq}}\text{OO}^{2+}$ by $\text{I}_2^{\bullet-}$. The other possibility, oxygen atom transfer of Scheme 13, is much more intriguing because this type of reactivity is rare for superoxometal complexes, and has been so far clearly identified only in the multistep reactions with NO which feature an intermediate peroxynitrito species [34,36].

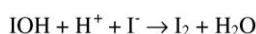
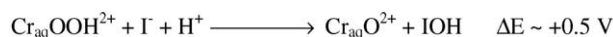
The existing potential data [102,103] for $\text{Cr}_{\text{aq}}\text{OO}^{2+}$ made it possible to estimate the thermodynamics in 1 M H^+ for the two paths in Schemes 12 and 13. The one-electron path, having $\Delta E = -0.13 \text{ V}$, is convincingly less favorable of the two, even though the 0.5 V value associated with the two-electron, oxygen atom transfer path, Scheme 13, is only an upper limit. Despite the clear thermodynamic advantage for oxygen atom transfer over electron transfer, the experimental data do not unambiguously support or rule out either mechanism.

3.3. Oxidation of bromide by $\text{Cr}_{\text{aq}}\text{O}^{2+}$

As expected, there is no reaction between $\leq 0.1 \text{ M Cl}^-$ and $\text{Cr}_{\text{aq}}\text{O}^{2+}$ during the short lifetime of $\text{Cr}_{\text{aq}}\text{O}^{2+}$ ($\leq 1 \text{ min}$ under most conditions). The oxidation of I^- , on the other hand, proved too fast to measure by either conventional or stopped-flow spectrophotometry, but the Br^- reaction was conveniently monitored by both techniques and utilized the superoxochromium ion as a kinetic probe [104].

No independent spectroscopic evidence exists for the protonated form of chromyl(IV) ion, $\text{Cr}_{\text{aq}}\text{OH}^{3+}$, in acidic solutions. Previous kinetic evidence existed only for the deprotonation of one of coordinated waters which results in inverse $[\text{H}^+]$ dependence for bimolecular decay of $\text{Cr}_{\text{aq}}\text{O}^{2+}$ [84]. Two key mechanistic questions were thus addressed in a study of the $\text{Cr}_{\text{aq}}\text{O}^{2+}/\text{Br}^-$ reaction: the availability of a proton-assisted pathway, and the preference for one-electron versus two-electron mechanism.

The decrease in the lifetime of $\text{Cr}_{\text{aq}}\text{O}^{2+}$ [29,84] with decreasing acid concentration severely limits the range of $[\text{H}^+]$ concentrations that can be used in kinetic studies. In the reaction with bromide $[\text{H}^+]$ was varied only between 0.10 and 0.21 M. For this set of conditions, the reaction exhibited a clean first-order dependence on $[\text{H}^+]$, as shown in Fig. 4 and the rate law in Eq.



Scheme 13.

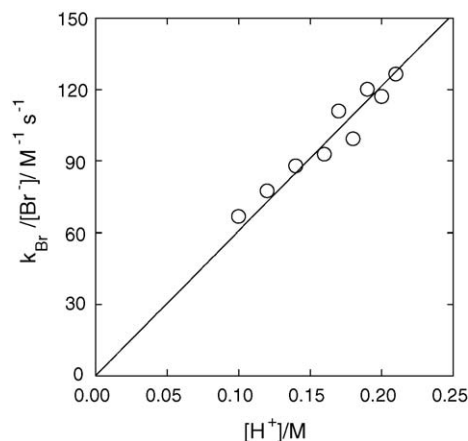


Fig. 4. Acid dependence of the second-order rate constant for the oxidation of Br^- by $\text{Cr}_{\text{aq}}\text{O}^{2+}$. Reproduced with permission from *Inorg. Chem.* 2005, 44, 9293–9298. © 2005 Am. Chem. Soc.

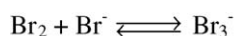
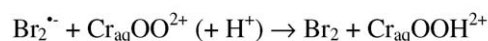
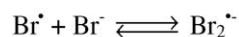
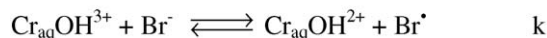
(25). Changing the solvent from H_2O to D_2O increased the rate constant, $k_{\text{H}}/k_{\text{D}} = 0.74$.

$$\frac{-d[\text{Cr}_{\text{aq}}\text{O}^{2+}]}{dt} = k_{25}[\text{Cr}_{\text{aq}}\text{O}^{2+}][\text{Br}^-][\text{H}^+] = k_{\text{Br}}[\text{Cr}_{\text{aq}}\text{O}^{2+}] \quad (25)$$

All of the data support the one-electron mechanism in Scheme 14. The derived rate law of Eq. (26) reduces to the observed form (Eq. (25)) upon introducing the inequality $[\text{H}^+] \ll K_{\text{a}}$. According to this interpretation, the rate constant k_{25} is the ratio k/K_{a} , and $[\text{Cr(IV)}]_{\text{tot}}$ is the sum of the concentrations of $\text{Cr}_{\text{aq}}\text{O}^{2+}$ and $\text{Cr}_{\text{aq}}\text{OH}^{3+}$. Estimates of the driving force for one-electron ($\Delta G \leq 19 \text{ kJ/mol}$) and two-electron ($\Delta G \leq 140 \text{ kJ/mol}$) pathways also heavily favor the one-electron alternative. Most importantly, the two-electron path was ruled out experimentally by demonstrating that $\text{Cr}_{\text{aq}}^{2+}$ was not involved as an intermediate.

$$\frac{-d[\text{Cr}_{\text{aq}}\text{O}^{2+}]}{dt} = k \frac{[\text{H}^+]}{K_{\text{a}} + [\text{H}^+]} [\text{Br}^-][\text{Cr(IV)}]_{\text{tot}} \quad (26)$$

In the proposed scheme, the first-order dependence on H^+ arises from prior protonation of $\text{Cr}_{\text{aq}}\text{O}^{2+}$. The large value of K_{a} , required by the rate law and consistent with the lack of experimental observation of $\text{Cr}_{\text{aq}}\text{OH}^{3+}$, comes as no surprise. Other metal(IV) oxo complexes of the first transition series for which data are available, e.g. $\text{V}_{\text{aq}}\text{O}^{2+}$ [105] and $\text{Ti}_{\text{aq}}\text{O}^{2+}$ [106],



Scheme 14.

Table 4
Summary of the rate constants for oxidation reactions with $\text{Cr}_{\text{aq}}\text{O}^{2+}$ ^a

Reductant	$\text{Cr}_{\text{aq}}\text{O}^{2+}$		$\text{Cr}_{\text{aq}}\text{OO}^{2+}$		
	k_0 ($\text{M}^{-1} \text{s}^{-1}$)	k_{H} ($\text{M}^{-2} \text{s}^{-1}$)	k_0 ($\text{M}^{-1} \text{s}^{-1}$)	k_{H} ($\text{M}^{-2} \text{s}^{-1}$)	E^{ob}
Br^-	~ 0	608	~ 0	~ 0	1.92 [109]
$\text{Ru}(\text{bpy})_3^{2+}$	< 10		^c		1.26 [108]
$\text{Os}(\text{phen})_3^{2+}$	1.37×10^3	1.94×10^3	17.5	221	0.84 [112]
$\text{HABTS}^-/\text{ABTS}^{2-}$	7.9×10^4 ^d		1.36×10^3 ^d		0.81 ^{e,f} /0.68 ^{f,g} [113]
$(\text{NH}_3)_5\text{Rupy}^{2+}$		$> 10^7$	7.0×10^4 ^h	1.78×10^5 ^h	0.305 [115]

^a At $25.0 \pm 0.2^\circ \text{C}$.

^b One-electron reduction potential (vs. NHE) for the reductant.

^c Ref [42] ^cNot determined.

^d Second-order rate constants in 0.10 M HClO_4 . Data from Ref. [116].

^e For $\text{ABTS}^{\bullet-}/\text{HABTS}^-$.

^f $\text{p}K_{\text{a}}$ ($\text{HABTS}^-/\text{ABTS}^{2-}$) = 2.2.

^g For $\text{ABTS}^{\bullet-}/\text{ABTS}^{2-}$.

^h Ref [101]. Reproduced with permission from *Inorg. Chem.* 2005, 44, 9293–9298. © 2005 Am. Chem. Soc.

also exhibit very small protonation constants, and in the case of $\text{Fe}_{\text{aq}}\text{O}^{2+}$ no evidence for protonation exists at pH 1–2 [107].

In comparison with other known oxidation reactions by $\text{Cr}_{\text{aq}}\text{O}^{2+}$, Table 4, the reaction with Br^- is inordinately fast. For example, there is no reaction between $\text{Cr}_{\text{aq}}\text{O}^{2+}$ and $\text{Ru}(\text{bpy})_3^{2+}$ ($k < 10 \text{ M}^{-1} \text{s}^{-1}$ in 0.1 M $\text{CF}_3\text{SO}_3\text{H}$), even though this complex is a much better 1-electron reductant ($E_{\text{Ru(III)/Ru(II)}} = 1.26 \text{ V}$) [108] than Br^- is (E for $\text{Br}^\bullet/\text{Br}^- = 1.92 \text{ V}$) [109], and the electron-exchange rate constant for the ruthenium couple is almost certainly greater than that for $\text{Br}^\bullet/\text{Br}^-$. A simple Marcus treatment [110,111] places the expected rate constant for the reaction with $\text{Ru}(\text{bpy})_3^{2+}$ more than six orders of magnitude above that for Br^- . Moreover, the reaction with $\text{Os}(\text{phen})_3^{2+}$ ($k = 1.94 \times 10^3 \text{ M}^{-2} \text{s}^{-1}$) is only about three times faster than the bromide reaction, even though the osmium complex is more strongly reducing than Br^- by close to 1.1 V [112]. The anionic $\text{HABTS}^-/\text{ABTS}^{2-}$ ($\text{p}K_{\text{a}} = 2.2$, $E = 0.68$ – 0.81 V , depending on $[\text{H}^+]$) [113] reacts only slightly faster than $\text{Os}(\text{phen})_3^{2+}$, and $(\text{NH}_3)_5\text{Rupy}^{2+}$ ($E = 0.305 \text{ V}$) [114] has $k > 10^7 \text{ M}^{-1} \text{s}^{-1}$ in 0.10 M HClO_4 . All the reductants, with the exception of Br^- , present a consistent reactivity picture.

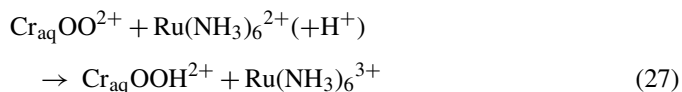
Rate constants for outer-sphere electron transfer that are smaller than calculated by Marcus theory can be attributed to a small transmission coefficient [111]. There is no provision, however, for reactions that are orders of magnitude faster than predicted. Such cases require a change in mechanism, most commonly to inner-sphere electron transfer between two metal complexes. There is no recognized, well-developed counterpart to this mechanism in the reactions between a non-metal and a metal complex, such as the $\text{Cr}_{\text{aq}}\text{O}^{2+}/\text{Br}^-$ reaction, but other examples of anomalously fast reactions of this kind have been reported [117–119]. The data have been rationalized by a strong overlap mechanism [117–119] that could function similar to an inner-sphere path.

In qualitative terms, this type of a mechanism would seem well suited for the present case as shown by the analysis of the data in Table 4. The most distinguishing feature that sets Br^- apart from all the other reductants in Table 4 is the ability of Br^- to coordinate to the metal.

Clearly, the driving force for the oxidation of $\text{Os}(\text{phen})_3^{2+}$ or $\text{HABTS}^-/\text{ABTS}^{2-}$ by $\text{Cr}_{\text{aq}}\text{O}^{2+}$ (E for $\text{Cr}_{\text{aq}}\text{O}^{2+}/\text{Cr}_{\text{aq}}^{3+} \geq 1.7 \text{ V}$) is extremely large, and the electron exchange rate constants for both reductants are close to diffusion-limited. The low observed rates must therefore reside in an extremely unfavorable term arising from small electron exchange rate constants and reduction potentials for the Cr(IV)/(III) couple in the appropriate hydrolytic states ($\text{Cr}^{\text{IV}}_{\text{aq}}\text{O}^{2+}/\text{Cr}^{\text{III}}_{\text{aq}}\text{O}^+$ and $\text{Cr}^{\text{IV}}_{\text{aq}}\text{OH}^{3+}/\text{Cr}^{\text{III}}_{\text{aq}}\text{OH}^{2+}$ for the acid-independent and acid-catalyzed terms), and the small protonation constant for $\text{Cr}_{\text{aq}}\text{O}^{2+}$. It would seem that prior association of Br^- with $\text{Cr}_{\text{aq}}\text{O}^{2+}$ (or $\text{Cr}_{\text{aq}}\text{OH}^{3+}$) would benefit the reaction by providing both a better orbital overlap and an intermediate with a finite lifetime to facilitate hydrolysis.

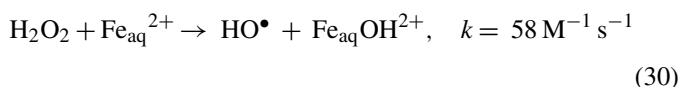
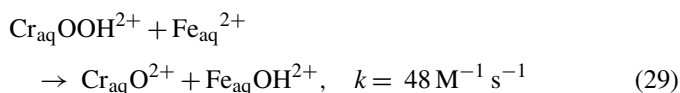
4. Reactions with transition metal complexes

Most of this chemistry has been reviewed earlier [29,42] and only a brief summary will be given here. One-electron reductions of superoxo complexes with outer-sphere reductants, such as $\text{Ru}(\text{NH}_3)_6^{2+}$, generate the corresponding hydroperoxides, Eq. (27) [69,120]. Such reactions have proved to be one of the best preparative routes to a number of hydroperoxo complexes. Inner-sphere reactions, on the other hand, involve bimetallic peroxo intermediates which eventually decompose to stable final products, Eq. (28) [69,120–124].



Transient metal(IV) oxo intermediates are generated in Fenton-like chemistry, Eq. (29), between the hydroperoxo complexes and substitutionally labile one-electron reductants. Rate constants for these reactions are remarkably similar to those observed for the reactions of H_2O_2 with the same reductants [74,125,126]. Oxygen atom transfer, on the other

hand, is significantly faster for the hydroperoxometal complexes as shown in previous sections and in some earlier work [29,74,90].

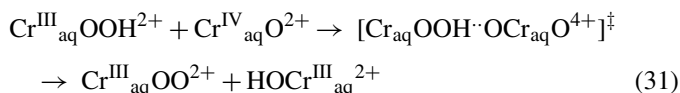


Kinetics of one-electron reductions of hydroperoxo complexes are typically independent of $[\text{H}^+]$. Oxidation reactions, on the other hand, often exhibit a term that is inversely proportional to the acid concentration, as in the case of $\text{L}^1(\text{H}_2\text{O})\text{CoOOH}^{2+}$ oxidation by IrCl_6^{2-} , $\text{Ru}(\text{bpy})_3^{3+}$, and $\text{Fe}_{\text{aq}}^{3+}$ [126]. The reaction with VO_2^+ is exceptional in that it is $[\text{H}^+]$ catalyzed, an observation that is easily understood in view of the demand for hydrogen ions as the dioxovanadium(V) is reduced to oxovanadium(IV) ion.

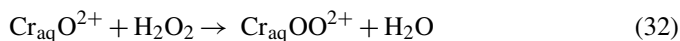
5. Cross-reactions between metal-oxo, hydroperoxo, and superoxo complexes

In metal-catalyzed oxidation reactions with molecular oxygen, both metal- and substrate-derived intermediates are involved. Directly or indirectly, such intermediates are usually pictured as leading to products, but other, potentially important reactions, must also be considered. There is an abundance of data on cross-reactions, self-reactions, and various other reactivity modes of alkyl peroxy radicals, alkoxy radicals, organic peroxides, and other intermediates derived from organic substrates. In contrast, very little information is available for the reactions between organic and metal-based intermediates [127,128], or between different types of metal-derived intermediates, even though some of them may be quite persistent and realistically involved in cross-reactions.

An example is provided by the ready oxidation of $\text{Cr}_{\text{aq}}\text{OOH}^{2+}$ by $\text{Cr}_{\text{aq}}\text{O}^{2+}$, $k = 1.34 \times 10^3 \text{ M}^{-1} \text{ s}^{-1}$ in 0.10 M HClO_4 [74]. The reaction generates $\text{Cr}_{\text{aq}}\text{OO}^{2+}$, easily recognized by its unique UV–vis spectrum. In D_2O , the rate constant is much smaller, $266 \text{ M}^{-1} \text{ s}^{-1}$. Even though some of the effect may be associated with the change of solvent from H_2O to D_2O , the observed $k_{\text{H}}/k_{\text{D}}$ is large enough to suggest hydrogen atom transfer as a kinetic step, Eq. (31).



The reaction between $\text{Cr}_{\text{aq}}\text{O}^{2+}$ and free H_2O_2 also generates $\text{Cr}_{\text{aq}}\text{OO}^{2+}$ [129], even in the absence of molecular oxygen, Eq. (32). This finding rules out the intermediacy of $\text{Cr}_{\text{aq}}^{2+}$ and its reaction with O_2 as the source of $\text{Cr}_{\text{aq}}\text{OO}^{2+}$, a mechanism known to be adopted by aliphatic alcohols, aldehydes, and carboxylic acids [29].

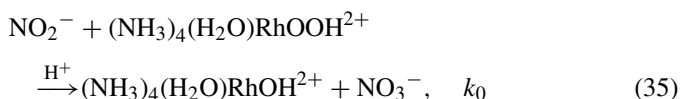
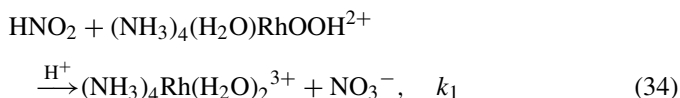
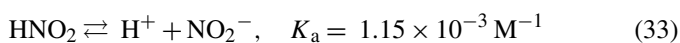


The rate constant for reaction (32), $k = 190 \text{ M}^{-1} \text{ s}^{-1}$, is somewhat smaller than that observed for the oxidation of $\text{Cr}_{\text{aq}}\text{OOH}^{2+}$ in Eq. (31). The activation parameters for reaction (32), $\Delta S^\ddagger = -116 \text{ J mol}^{-1} \text{ K}^{-1}$, $\Delta H^\ddagger = 25 \text{ kJ mol}^{-1}$, indicate a highly structured transition state and compensating bond-making and bond-breaking processes. A mechanism consistent with all the data, including the observed kinetic isotope effect, $k_{\text{H}}/k_{\text{D}} = 3.6$, features either hydrogen atom or hydride transfer from coordinated H_2O_2 to $\text{Cr}_{\text{aq}}\text{O}^{2+}$.

6. Acid catalysis in reductions of metal-activated oxygen

It should not be too surprising that H^+ catalyzes oxidation reactions of halides by superoxo, hydroperoxo, and oxo complexes, although the complete absence of an acid-independent term in the rate law may not have been fully expected. In all the cases, the overall stoichiometry requires hydrogen ions, and the rate determining steps are strongly endothermic. Thus the protonation of the oxidant prior to electron or oxygen atom transfer facilitates the reaction and provides a better path and kinetics for the reaction. As suggested by this analysis, reactions with substrates other than halide ions are also acid catalyzed. Prominent among them is the oxidation of several organic sulfides, a thiolato cobalt complex $(\text{en})_2\text{Co}(\text{SCH}_2\text{CH}_2\text{NH}_2)^{2+}$, as well as triaryl phosphines, for which oxygen atom transfer has been confirmed by isotopic labeling [98].

Nitrite provides a particularly illustrative example of acid catalyzed-oxidation, Eqs. (33)–(35). The complex $[\text{H}^+]$ -dependence arises from a combination of the acid–base equilibrium relating NO_2^- and HNO_2 , coupled to a first-order term in $[\text{H}^+]$ for each of the forms, $k_0 = 1.54 \times 10^4 \text{ M}^{-2} \text{ s}^{-1}$, $k_1 = 8.91 \times 10^2 \text{ M}^{-2} \text{ s}^{-1}$.



Similarly, the oxidation of hydrazinium ion by $\text{Cr}_{\text{aq}}\text{OO}^{2+}$ in acidic solutions obeys the rate law, $-d[\text{Cr}_{\text{aq}}\text{OO}^{2+}]/dt = 50.4 [\text{N}_2\text{H}_5^+] [\text{H}^+][\text{Cr}_{\text{aq}}\text{OO}^{2+}]$ [130]. The catalysis by H^+ was explained by prior protonation of the superoxo complex. In the other, much less satisfactory option, the reduction would be carried out by the weak and typically unreactive $\text{N}_2\text{H}_6^{2+}$.

The effect of H^+ on outer-sphere electron transfer reductions of superoxo complexes has been examined in only a limited number of cases. In some of them, H^+ has a strong accelerating effect, but an acid-independent path often competes, and sometimes even dominates the kinetics, as shown in Table 4. In general terms such behavior can be rationalized by the large span in the driving force for these reactions, such that in some cases even an acid-independent path becomes thermodynamically accessible and kinetically competent.

7. Conclusions

The deceptively simple reactions between transition metal-activated oxygen and inorganic substrates are excellent mechanistic models for biological and laboratory oxidation reactions. The often-neglected effect of the metal on acid–base chemistry at oxygen, combined with acid–base chemistry elsewhere in the complex, opens new mechanistic routes and/or accelerates those already available to the system. As a result, inorganic substrates utilize a variety of pathways, including some that are more frequently associated with the oxidation of organic substrates, i.e. hydrogen atom and oxygen atom transfers.

Some of the reactions of simple mononuclear inorganic complexes with inorganic substrates have many features in common with enzymatic oxygen activation (such as that in cytochrome P450-mediated processes), chemistry of haloperoxidases, and certain steps in oxygen-evolution in photosystem II. Studies of small, well-defined models or prototypes can provide invaluable clues about the functioning of known, complex processes, and help design new catalytic reactions to utilize the great oxidizing power of oxygen.

Acknowledgements

The dedication and hard work of all of my associates whose work is described in this article are gratefully acknowledged. Our work was supported by the U.S. Department of Energy, Office of Basic Energy Sciences, Division of Chemical Sciences under Contract W-7405-ENG-82 with Iowa State University, and by National Science Foundation (grants CHE-9303388 and CHE-9982004).

References

- [1] P.R.O. De Montellano, J.J. De Voss, *Nat. Prod. Rep.* 19 (2002) 477.
- [2] A. Decker, E.I. Solomon, *Curr. Opin. Chem. Biol.* 9 (2005) 152.
- [3] J.T. Groves, *Proc. Natl. Acad. Sci. U.S.A.* 100 (2003) 3569.
- [4] D.A. Kopp, S.J. Lippard, *Curr. Opin. Chem. Biol.* 6 (2002) 568.
- [5] T.M. Makris, R. Davydov, I.G. Denisov, B.M. Hoffman, S.G. Sligar, *Drug Metab. Rev.* 34 (2002) 691.
- [6] P.J. O'Brien, *Chem.-Biol. Interact.* 129 (2000) 113.
- [7] T.D.H. Bugg, *Curr. Opin. Chem. Biol.* 5 (2001) 550.
- [8] G. Strukul (Ed.), *Catalytic Oxidations with Hydrogen Peroxide as Oxidant*, Kluwer Academic Publishers, Dordrecht, 1992.
- [9] Y. Ishii, S. Sakaguchi, T. Iwahama, *Adv. Synth. Catal.* 343 (2001) 393.
- [10] L.I. Simandi, *Proceedings of the 4th International Symp. on Dioxygen Activation and Homogeneous Catalytic Oxidation*, 1991.
- [11] R.K. Grasselli, S.T. Oyama, A.M. Gaffney, J.E. Lyons (Eds.), *Third World Congress on Oxidation Catalysis*, Elsevier, Amsterdam, 1997.
- [12] D.F.V. Lewis, *J. Chem. Technol. Biotechnol.* 77 (2002) 1095.
- [13] P.I. Moreira, C.R. Oliveira, M.S. Santos, A. Nunomura, K. Honda, X. Zhu, M.A. Smith, G. Perry, *Curr. Neurovasc. Res.* 2 (2005) 179.
- [14] N. Ohnishi, S.I. Allakhverdiev, S. Takahashi, S. Higashi, M. Watanabe, Y. Nishiyama, N. Murata, *Biochemistry* 44 (2005) 8494.
- [15] G. Williamson, C. Manach, *Am. J. Clin. Nutr.* 81 (2005) 243S.
- [16] A.J. Young, D.M. Phillip, G.M. Lowe, *Oxid. Stress Dis.* 13 (2004) 105.
- [17] G. Duthie, P. Gardner, J. Kyle, D. McPhail, *ACS Symp. Ser.* 871 (2004) 90.
- [18] J. Grassmann, S. Hippeli, E.F. Elstner, *Plant Physiol. Biochem. (Paris France)* 40 (2002) 471.
- [19] B. Halliwell, J. Rafter, A. Jenner, *Am. J. Clin. Nutr.* 81 (2005) 268S.
- [20] S. Hippeli, E.F. Elstner, *Free Rad. Res.* 31 (1999) S81.
- [21] S. Hippeli, E.F. Elstner, *FEBS Lett.* 443 (1999) 1.
- [22] K.M. Janisch, J. Milde, H. Schempp, E.F. Elstner, *Dev. Ophthalmol.* 38 (2005) 59.
- [23] C. Tommos, C.W. Hoganson, M.D. Valentin, N. Lydakis-Simantiris, P. Dorlet, K. Westphal, H.A. Chu, J. McCracken, G.T. Babcock, *Curr. Opin. Chem. Biol.* 2 (1998) 244.
- [24] A.W. Rutherford, A. Boussac, P. Faller, *Biochim. Biophys. Acta* 1655 (2004) 222.
- [25] J.H. Nugent, A.M. Rich, M.C. Evans, *Biochim. Biophys. Acta* 1503 (2001) 138.
- [26] C.W. Hoganson, C. Tommos, *Biochim. et Biophys. Acta Bioenerget.* 1655 (2004) 116.
- [27] C.W. Hoganson, G.T. Babcock, *Science* 277 (1997) 1953.
- [28] M. Sjoedin, S. Styring, B. Akermark, L. Sun, L. Hammarstrom, *Philos. Trans. R. Soc. Lond. Ser. B: Biol. Sci.* 357 (2002) 1471.
- [29] A. Bakac, *Prog. Inorg. Chem.* 43 (1995) 267.
- [30] M.P. Doyle, J.W. Hoekstra, *J. Inorg. Biochem.* 14 (1981) 351.
- [31] M.P. Doyle, J.G. Herman, R.L. Dykstra, *J. Free Rad. Biol. Med.* 1 (1985) 145.
- [32] S.S. Marla, J. Lee, J.T. Groves, *Proc. Natl. Acad. Sci. U.S.A.* 94 (1997) 14243.
- [33] R. Shimanovich, J.T. Groves, *Arch. Biochem. Biophys.* 387 (2001) 307.
- [34] O. Pestovsky, A. Bakac, *J. Am. Chem. Soc.* 124 (2002) 1698.
- [35] O. Pestovsky, A. Bakac, *Inorg. Chem.* 41 (2002) 901.
- [36] A. Nemes, O. Pestovsky, A. Bakac, *J. Am. Chem. Soc.* 124 (2002) 421.
- [37] L.J. Ignarro (Ed.), *Nitric Oxide. Biology and Pathobiology*, Academic, San Diego, 2000.
- [38] G.L. Squadrito, W.A. Pryor, *Free Rad. Biol. Med.* 25 (1998) 392.
- [39] J.S. Beckman, W.H. Koppenol, *Am. J. Physiol.* 271 (1996) C1424.
- [40] S. Goldstein, J. Lind, G. Merenyi, *Chem. Rev.* 105 (2005) 2457.
- [41] S. Herold, W.H. Koppenol, *Coord. Chem. Rev.* 249 (2005) 499.
- [42] A. Bakac, *Adv. Inorg. Chem.* 55 (2004) 1.
- [43] A. Marchaj, A. Bakac, J.H. Espenson, *Inorg. Chem.* 31 (1992) 4164.
- [44] A. Bakac, J.H. Espenson, *Inorg. Chem.* 29 (1990) 2062.
- [45] A. Bakac, T.J. Won, J.H. Espenson, *Inorg. Chem.* 35 (1996) 2171.
- [46] R. Wever, B.E. Krenn (Eds.), *Vanadium in Biological Systems*, Kluwer, Boston, 1990.
- [47] B. Meunier, in: G. Strukul (Ed.), *Catalytic oxidations with Hydrogen Peroxide as Oxidant*, Kluwer, Boston, 1992, p. 153.
- [48] V. Conte, F. Difuria, G. Modena, in: W. Ando (Ed.) *Organic Peroxides*, Wiley, Chichester, 1992.
- [49] T. Kratz, W. Zeiss, in: W. Adam (Ed.), *Peroxide Chemistry. Mechanistic and Preparative Aspects of Oxygen Transfer*, Wiley-VCH, Weinheim, 2000, p. 39.
- [50] C. Slebodnick, N.A. Law, V.L. Pecoraro, in: B. Meunier (Ed.), *Biomimetic Oxidations Catalyzed by Transition Metal Complexes*, Imperial College Press, London, 2000.
- [51] J.W. Sam, X.-J. Tang, J. Peisach, *J. Am. Chem. Soc.* 116 (1994) 5250.
- [52] R.J. Guajardo, J.D. Tan, P.K. Mascharak, *Inorg. Chem.* 33 (1994) 2838.
- [53] A.J. Simaan, F. Banse, P. Mialane, A. Boussac, S. Un, T. Kargar-Grisel, G. Bouchoux, J.J. Girerd, *Eur. J. Chem.* (1999) 993.
- [54] K.B. Jensen, C.J. McKenzie, L.P. Nielsen, J.Z. Pedersen, H.M. Svendsen, *Chem. Commun.* (1999) 1313.
- [55] Y. Takahashi, M. Hashimoto, S. Hikichi, M. Akita, Y. Moro-oka, *Angew. Chem. Int. Ed.* 38 (1999) 3074.
- [56] R.Y.N. Ho, G. Roelfes, R. Hermant, R. Hage, B.L. Feringa, L. Que Jr., *Chem. Commun.* (1999) 2161.
- [57] A.F.M.M. Rahman, W.G. Jackson, A.C. Willis, *Inorg. Chem.* 43 (2004) 7558.
- [58] M. Ibrahim, I.G. Denisov, T.M. Makris, J.R. Kincaid, S.G. Sligar, *J. Am. Chem. Soc.* 125 (2003) 13714.
- [59] I.G. Denisov, T.M. Makris, S.G. Sligar, *J. Biol. Chem.* 277 (2002) 42706.

- [60] H. Suzuki, S. Matsuura, Y. Moro-oka, T. Ikawa, *J. Organomet. Chem.* 286 (1985) 247.
- [61] F. Igersheim, H. Mimoun, *Nouv. J. Chim.* 4 (1980) 711.
- [62] A.J. Simaan, S. Dopner, F. Banse, S. Bourcier, G. Bouchoux, A. Bous-sac, P. Hildebrandt, J.-J. Girerd, *Eur. J. Inorg. Chem.* (2000) 1627.
- [63] O. Horner, C. Jeandey, J.-L. Oddou, P. Bonville, C.J. McKenzie, J.-M. Latour, *Eur. J. Inorg. Chem.* (2002) 3278.
- [64] M.R. Bukowski, P. Comba, C. Limberg, M. Merz, L. Que Jr., T. Wis-tuba, *Angew. Chem., Int. Ed.* 43 (2004) 1283.
- [65] A.J. Simaan, F. Banse, J.-J. Girerd, K. Wieghardt, E. Bill, *Inorg. Chem.* 40 (2001) 6538.
- [66] E. Kim, E.E. Chufan, K. Kamaraj, K.D. Karlin, *Chem. Rev.* 104 (2004) 1077.
- [67] T. Osako, S. Nagatomo, Y. Tachi, T. Kitagawa, S. Itoh, *Angew. Chem., Int. Ed.* 41 (2002) 4325.
- [68] M.M. Konnick, I.A. Guzei, S.S. Stahl, *J. Am. Chem. Soc.* 126 (2004) 10212.
- [69] K. Kumar, J.F. Endicott, *Inorg. Chem.* 23 (1984) 2447.
- [70] I.A. Guzei, A. Bakac, *Inorg. Chem.* 40 (2001) 2390.
- [71] M. Vasbinder, A. Bakac, unpublished observations, 2005.
- [72] G. Pregaglia, D. Morelli, F. Conti, G. Gregorio, R. Ugo, *Disc. Faraday Soc.* (1968) 110.
- [73] D.D. Wick, K.I. Goldberg, *J. Am. Chem. Soc.* 121 (1999) 11900.
- [74] W.-D. Wang, A. Bakac, J.H. Espenson, *Inorg. Chem.* 32 (1993) 5034.
- [75] V.V. Rostovtsev, L.M. Henling, J.A. Labinger, J.E. Bercaw, *Inorg. Chem.* 41 (2002) 3608.
- [76] A.W. Bushnell, G.C. Lalor, E.A. Moelwyn-Hughes, *J. Chem. Soc., A* (1966) 719.
- [77] G.C. Lalor, J. Lang, *J. Chem. Soc.* (1963) 5620.
- [78] S.A. Mirza, B. Bocquet, C. Robyr, S. Thomi, A.F. Williams, *Inorg. Chem.* 35 (1996) 1332.
- [79] G.V. Buxton, F. Djouider, *J. Chem. Soc., Faraday Trans.* 92 (1996) 4173.
- [80] A. Bakac, W.-D. Wang, *J. Am. Chem. Soc.* 118 (1996) 10325.
- [81] A. Bakac, W.-D. Wang, *Inorg. Chim. Acta* 297 (2000) 27.
- [82] O. Pestovsky, A. Bakac, *Dalton Trans.* (2005) 556.
- [83] K. Lemma, A. Ellern, A. Bakac, *Dalton Trans.* (2006) 58.
- [84] A. Nemes, A. Bakac, *Inorg. Chem.* 40 (2001) 2720.
- [85] C.W. Hoganson, G.T. Babcock, *Science* 277 (1997) 1953.
- [86] V.L. Pecoraro, M.J. Baldwin, M.T. Caudle, W.-Y. Hsieh, N.A. Law, *Pure Appl. Chem.* 70 (1998) 925.
- [87] K.L. Westphal, C. Tommos, R.I. Cukier, G.T. Babcock, *Curr. Opin. Plant Biol.* 3 (2000) 236.
- [88] K. Lemma, A. Bakac, *Inorg. Chem.* 43 (2004) 4505.
- [89] M. Eigen, K. Kustin, *J. Am. Chem. Soc.* 84 (1962) 1355.
- [90] A. Bakac, B. Assink, J.H. Espenson, W.-D. Wang, *Inorg. Chem.* 35 (1996) 788.
- [91] W.C. Bray, R.S. Livingston, *J. Am. Chem. Soc.* 45 (1923) 1251.
- [92] J.H. Espenson, O. Pestovsky, P. Huston, S. Staudt, *J. Am. Chem. Soc.* 116 (1994) 2869.
- [93] H. Taube, *J. Am. Chem. Soc.* 64 (1942) 2468.
- [94] R.C. Beckwith, T.X. Wang, D.W. Margerum, *Inorg. Chem.* 35 (1996) 995.
- [95] U. von Gunten, Y. Oliveras, *Water Res.* 31 (1997) 900.
- [96] A. Butler, A.H. Baldwin, *Struct. Bond. (Berlin)* 89 (1997) 109.
- [97] G.J. Colpas, B.J. Hamstra, J.W. Kampf, V.L. Pecoraro, *J. Am. Chem. Soc.* 118 (1996) 3469.
- [98] K. Lemma, A. Bakac, *Inorg. Chem.* 43 (2004) 6224.
- [99] R.W. Alder, M.C. Whiting, *J. Chem. Soc.* (1964) 4707.
- [100] T.J. Lewis, D.H. Richards, D.A. Salter, *J. Chem. Soc.* (1963) 2434.
- [101] A. Bakac, C. Shi, O. Pestovsky, *Inorg. Chem.* 43 (2004) 5416.
- [102] C. Kang, F.C. Anson, *Inorg. Chem.* 33 (1994) 2624.
- [103] J.H. Espenson, A. Bakac, J. Janni, *J. Am. Chem. Soc.* 116 (1994) 3436.
- [104] M. Hung, A. Bakac, *Inorg. Chem.* 44 (2005), Accepted.
- [105] I. Nagypal, I. Fabian, R.E. Connick, *Acta Chim. Acad. Scient. Hung.* 110 (1982) 447.
- [106] P. Comba, A. Merbach, *Inorg. Chem.* 26 (1987) 1315.
- [107] O. Pestovsky, S. Stoian, E.L. Bominaar, X. Shan, E. Münck, L.J. Que, A. Bakac, *Angew. Chem., Int. Ed.* 44 (2005) 6871.
- [108] C.-T. Lin, W. Bottcher, M. Chou, C. Creutz, N. Sutin, *J. Am. Chem. Soc.* 98 (1976) 6536.
- [109] D.M. Stanbury, *Adv. Inorg. Chem.* 33 (1989) 69.
- [110] R.A. Marcus, *J. Chem. Phys.* 43 (1965), 679, 2654.
- [111] N. Sutin, *Prog. Inorg. Chem.* 30 (1983) 441.
- [112] R. Sarala, S.B. Rabin, D.M. Stanbury, *Inorg. Chem.* 30 (1991) 3999.
- [113] S.L. Scott, W.-J. Chen, A. Bakac, J.H. Espenson, *J. Phys. Chem.* 97 (1993) 6710.
- [114] A.J. Bard, R. Parsons, J. Jordan, *Standard Potentials in Aqueous Solution*, Marcel Dekker, New York Basel, 1985.
- [115] A.J. Bard, R. Parsons, J. Jordan, *Standard Potentials in Aqueous Solution*, Marcel Dekker, New York Basel, 1985, p. 418.
- [116] S.L. Scott, A. Bakac, J.H. Espenson, *J. Am. Chem. Soc.* 114 (1992) 4205.
- [117] D.M. Stanbury, R. Martinez, E. Tseng, C.E. Miller, *Inorg. Chem.* 27 (1988) 4277.
- [118] Z. Toth, I. Fabian, *Inorg. Chem.* 39 (2000) 4608.
- [119] Z. Toth, I. Fabian, A. Bakac, *Inorg. React. Mech.* 3 (2001) 147.
- [120] M.E. Brynildson, A. Bakac, J.H. Espenson, *Inorg. Chem.* 27 (1988) 2592.
- [121] J.F. Endicott, K. Kumar, *ACS Symp. Ser.*, vol. 198, 1982, p. 425.
- [122] M. Munakata, J.F. Endicott, *Inorg. Chem.* 23 (1984) 3693.
- [123] C.-L. Wong, J.A. Switzer, K.P. Balakrishnan, J.F. Endicott, *J. Am. Chem. Soc.* 102 (1980) 5511.
- [124] C.-L. Wong, J.F. Endicott, *Inorg. Chem.* 20 (1981) 2233.
- [125] W.-D. Wang, A. Bakac, J.H. Espenson, *Inorg. Chem.* 32 (1993) 2005.
- [126] W.-D. Wang, A. Bakac, J.H. Espenson, *Inorg. Chem.* 34 (1995) 4049.
- [127] A. Bakac, *J. Am. Chem. Soc.* 124 (2002) 9136.
- [128] A. Bakac, *J. Am. Chem. Soc.* 124 (2002) 3816.
- [129] A.M. Al-Ajlouni, J.H. Espenson, A. Bakac, *Inorg. Chem.* 32 (1993) 3162.
- [130] S.L. Bruhn, A. Bakac, J.H. Espenson, *Inorg. Chem.* 25 (1986) 535.